

# Resource classification – a case study from the Joffre-hosted iron ore of BHP Billiton's Mount Whaleback operations

Chris De-Vitry

*It is recognised by the current JORC (1999) code that resource classification involves the interaction of numerous qualitative and quantitative criteria such as data quality, geological continuity and grade continuity. No prescribed criteria and rules will work for all situations or even between different ore types within the same deposit. Also, these criteria and rules are sometimes applied without a clear understanding of their appropriateness, accuracy or correct implementation. For these reasons, case studies are useful to evaluate and compare criteria commonly used to assist in resource classification. In this paper, blasthole data from a selected area of Joffre Member hosted ore of the Brockman Iron Formation at the Mount Whaleback orebody are used as the basis of a case study for the above-mentioned purposes.*

*Iron grade, in percent, is interpolated from a blasthole dataset into a block model using ordinary kriging. Samples are then removed from this blasthole dataset to produce a random sample grid, a semi-random sample grid and a regular sample grid. Block iron grades are obtained using nearest neighbour, inverse distance squared and ordinary kriging estimation methods and sequential gaussian simulation, using these three blasthole data subsets as inputs. This provides three groups of estimates and one group of simulations with the ordinary kriging estimate based on the complete blasthole dataset being considered to represent the true estimate of iron grades. Also generated during this process are measurements of the expected error for each block grade. These measures of error range from the simple, such as drill spacing, through to more advanced methodologies such as kriging efficiency and simulation. The grade and error determined from estimation and simulation are then compared to the true grade and true error using graphs and statistics. In order of increasing accuracy, the block grade*

*determination methods were nearest neighbour, inverse distance weighting, ordinary kriging and finally the average of multiple simulations. Simulation in some instances doubled the accuracy of individual block grades when compared to nearest neighbour and inverse distance weighting estimates. It was found that many methodologies for determining the error of individual block grades performed equally well with only methods such as average drillhole spacing and classification by search ellipse pass number performing poorly. An approach on how to convert the above-mentioned error determinations of individual blocks into a meaningful JORC classification is also discussed.*

*Although advanced non-linear resource estimates are applicable, most iron ore mines are still using relatively straightforward methods. The use of blasthole data and some simple linear estimation methods and simple linear-based error estimates makes this study repeatable for most iron ore sites and their resource geologists. This style of investigation is recommended as a useful approach for the competent person to apply to their deposit and thus better select, implement and understand the criteria used for resource classification and provide more consistency and confidence in the resource classification process.*

*Chris De-Vitry is a Senior Resource Geologist at BHP Billiton Iron Ore Pty Ltd, PO Box 655, Newman, WA 6753, Australia (E-mail: [chris.w.devitry@bhpbilliton.com](mailto:chris.w.devitry@bhpbilliton.com)). He will shortly move to MPI Mines, Stawell Gold Mine, P.O. Box 265 Stawell, 3380, Victoria, Australia.*

*© 2003 IoM Communications Ltd. Published by Maney for the Institute of Materials, Minerals and Mining in association with AusIMM. Manuscript received 9 September 2002; accepted in final form 5 May 2003.*

*Keywords: Resource classification, Mount Whaleback mine*

## INTRODUCTION

BHP Billiton Iron Ore Pty Ltd's Mount Whaleback mine is located 5 km west of the town of Newman in the South Eastern Pilbara region of Western Australia. The deposit occurs within the Brockman Iron Formation of the Hamersley Group. The Brockman Iron Formation as described by Kneeshaw<sup>11</sup> has been the most economically important formation in the Province with its (unenriched) thickness varying from 500–620 m. It is composed of an alternating sequence of banded iron

formation (BIF), shale and chert and is divided into four Members:

- (i) Dales Gorge Member (~150 m thick) – alternating assemblage of 17 BIF and 16 shale macrobands.
- (ii) Mount Whaleback Shale Member (~50 m thick) – a lower zone of four alternating macrobands of shale and BIF and an upper zone of numerous mesobands of chert and shale.
- (iii) Joffre Member (~360 m thick) – BIF sequence with only minor shale interbeds that are thinner

than those in the Dales Gorge Member.

- (iv) The Yandicoogina Shale Member (~60 m thick) – interbedded chert and shale.

**OVERVIEW OF THE METHODOLOGY**

This study uses a 9 x 15 m (with 1 centre hole) blasthole dataset from a single bench of the Whaleback open pit to interpolate (via ordinary kriging) iron grades into 20 x 20 m blocks. These grade estimates are considered reality. The 9 x 15 m blasthole data are subset into less densely sampled datasets and these are also used to estimate and simulate grades into the 20 x 20 m blocks (point simulations are averaged into blocks). Nearest neighbour, inverse distance squared, ordinary kriging and sequential gaussian simulation are used in the estimation and simulation. Various methodologies are used to determine the accuracy of block grades. All of the estimation, simulation and data analysis presented in this paper were generated using Datamine™ and Isatis™ software.

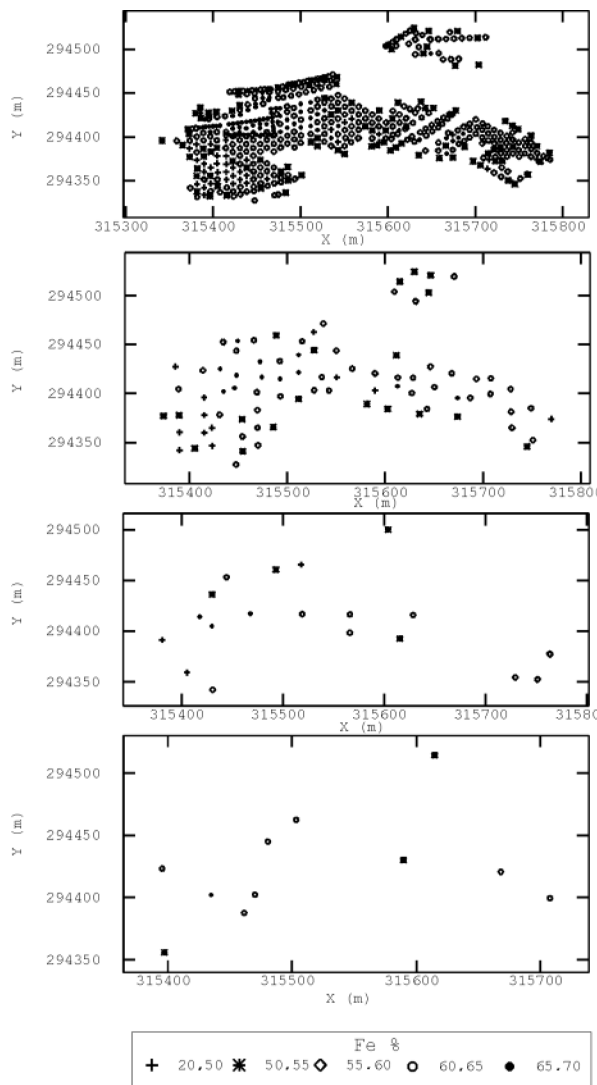
By comparing the assumed actual (reality) iron grades to the estimated or simulated iron grades and the assumed actual error to the error obtained from estimation or simulation, it can be understood how various error determination methodologies work when we try to estimate or simulate grades from wide spaced drillhole data into a block model.

The three sample data subsets were selected to be representative of some of the sample patterns and data densities found at actual iron ore projects. It is important to note that the three data subsets have different numbers of data with each dataset having different mean grades. This must be taken into account when examining the results. If the sample grades are not representative of the actual data, no estimation or simulation technique can compensate for this.

**DESCRIPTION OF THE DATASETS USED**

A bench (490 RL) of blasthole data from the Whaleback pit containing Joffre Member hosted ore was selected for this study. This bench contains blastholes on a 9 x 15 m (with 1 centre hole) grid with the sampled portion of each hole being 15 m. To differentiate ore and waste, a 50% iron cut-off was used. This boundary includes some material below cut-off which reflects the normal situation in which with wide-spaced drilling not all the below cut-off material can be domained separately. Although the datasets mentioned below are different, the interpreted ore/waste boundary is constant.

To obtain a 20 x 20 m regular sample grid, the blastholes closest to the centre of 20 x 20 m blocks were selected. To obtain a random, stratified grid, this process was repeated with a 40 x 40 m grid; however, in this situation, the blasthole sample was randomly selected from anywhere within each 40 x 40 m block. To create a random grid, blastholes were selected at random within the ore boundary. Plan views and basic statistics for these datasets are summarised in Fig. 1 and Table 1, respectively.



**1 Plans of the four datasets used in this study with symbols representing different percentages of iron. The upper plan represents all of the 9 x 15 m (with 1 hole centre hole) blasthole data, the upper-mid plan represents the regular data subset, the lower-mid plan represents the random stratified data subset and the lower plan represents the random data subset**

**OVERVIEW OF TECHNICAL TERMS USED**

**General terms**

Mean percentage difference is used to compare paired data (Eq. 1). When a cut-off grade is applied to a block model, the mean recovered grade should be approximately equal to the predicted mean grade, otherwise the estimate is conditionally biased.

$$200 * AV( ACT - EST ) / ( ACT + EST ) \tag{1}$$

where AV = absolute value, ACT = actual value, and EST = estimated value or the average of multiple simulations.

**Error determination methodologies**

Error determinations in this paper can be divided into three main groups: (i) those that can be applied to

**Table 1 Basic statistics of percent iron for the datasets used in this study. Note that regular, random stratified and random datasets are all subsets of the complete (all data) dataset**

Dataset	Number of samples	Minimum % Fe	Maximum % Fe	Mean % Fe	SD
All data	507	25.0	68.0	58.4	6.7
Regular	84	36.0	67.1	57.3	7.4
Random stratified	19	43.6	67.7	57.2	7.4
Random	11	50.0	65.6	59.9	5.0

inverse distance weighting; (ii) those techniques that can be applied to either ordinary kriging or inverse distance interpolation methodologies; and (iii) the standard deviation of multiple simulations.

#### *Inverse distance error estimation methodologies*

This group of error estimation methodologies that are possible with inverse distance interpolation consist of weighted distance, distance to the closest sample and the number of samples used in the resource estimate. The weighted distance is a weighted average of the sample to block distances or discretisation points, where the weights are those applied to samples during grade interpolation.

Both the weighted distance technique and the distance to the nearest sample can be applied to actual distances or distances transformed according to the search ellipse dimensions. Distance is treated as proportion between 0 and 1 with 1 representing the size of the search ellipse. In this way, anisotropy in grade continuity can be accounted for.

#### *Ordinary kriging error estimation methodologies*

The error estimation methodologies applied to ordinary kriging consist of kriging variance, kriging efficiency, slope of the regression between 'actual' and 'estimated' grades, the weighted average variogram and the modified variance.

Kriging variance is the estimated error variance produced during ordinary kriging. Kriging efficiency (Eq. 2) is directly linked to the kriging variance and the two have a correlation coefficient of 1. The kriging efficiency is a number between 0 and 1 with 1 representing a perfect estimate.

The slope of the regression between 'actual' and 'estimated' grades (Eq. 3) should give results close to the kriging efficiency as the two are closely correlated (Fig. 2).

$$KE = (BV - KV)/BV \quad (2)$$

$$R = (BV - KV + \mu)/(BV - KV + 2\mu) \quad (3)$$

where BV = theoretical variance of blocks within the domain, KV = kriging variance,  $\mu$  = the absolute value of the LaGrange multiplier for each parent cell, KE = kriging efficiency, and R = slope of the regression between 'actual' and 'estimated' grades.

The weighted average variogram is the average value of the sample weights used in interpolation multiplied by their corresponding variogram values.

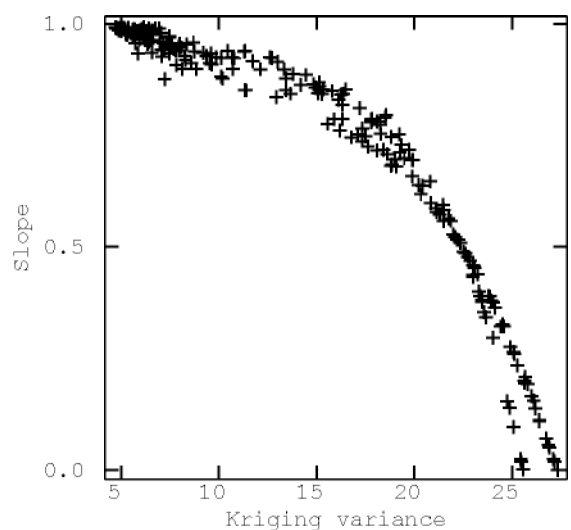
As discussed by Arik,<sup>1</sup> the combined variance is calculated via the square root of the kriging variance multiplied by the weighted sample to block variance (Eq. 4). This takes into account the data configuration as well as the variability of the values that have been used to estimate a block.

$$CV = \sqrt{(KV * S_w^2)} \quad (4)$$

where CV = combined variance, KV = kriging variance, and  $S_w^2$  = the weighted sample to block variance, where the weights are those used in the ordinary kriging interpolation.

#### *Sequential gaussian simulation*

Following multiple realisations, each simulated point (or points averaged into blocks) contains a distribution of possible grades. These distributions can be described via the conditional standard deviation, inter-quartile range, probabilities above a cut-off, etc. Simulation is a powerful tool for assessing uncertainty; however, in this case study, we have only used the conditional standard deviation. This was done to provide an error determination compatible with the error obtained from other linear estimation techniques discussed in this paper.



**2 Scatter-plot of slope of the regression between 'actual' and 'estimated' grades versus kriging variance. This scatter-plot includes block grades interpolated from the regular, random and random stratified datasets**

## VARIOGRAPHY, GAUSSIAN TRANSFORMATIONS AND OPTIMISING THE SAMPLE SEARCH STRATEGY

### Generation of variograms and variogram fitting

#### Variograms of percent iron grade

Six horizontal directional variograms (variograms are calculated as half the average squared difference between the paired data values) were calculated with a 10 m lag using all the 9 x 15 m (with 1 hole centre hole) blasthole data. As can be seen in Fig. 3, these variograms have a very low nugget and a pronounced anisotropy with the greatest continuity being east–west and the lowest continuity being north–south. These variograms were fitted using a three structure spherical model (Table 2).

#### Variograms based on percent iron grade transformed to a gaussian distribution

A frequency inversion with 50 hermite polynomials was used to transform the percent iron grades into a gaussian distribution. Because the datasets are small, the maximum and minimum percent iron values do not reflect all the possibilities. The maximum and minimum allowable iron grades (back transformed) were set identical to the full 9 x 15 m (with 1 hole centre hole) blasthole dataset. All of the four datasets were transformed to gaussian distributions in this way.

It could be argued that setting the minimum and maximum values to that of the full dataset is unduly favourable for the conditional simulation. For many commodities (e.g. gold), this would be so; however, in this ore type, the maximum and minimum iron grades are well known.

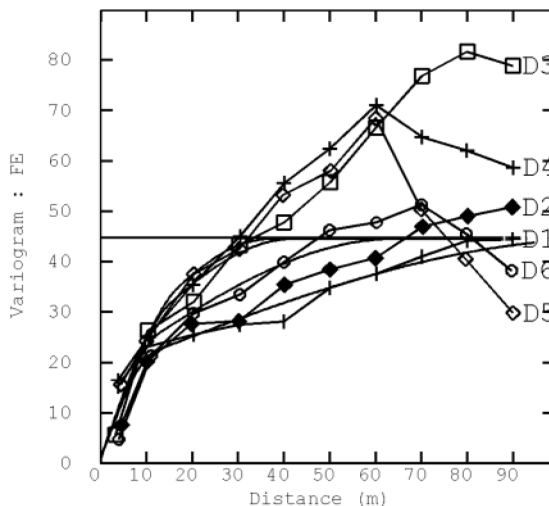
Six variograms based on the gaussian transformed percent iron grade (using all the data) were generated with the same parameters as those mentioned above. Often, especially with nuggetty, highly skewed datasets, the gaussian transformed variable will produce better variograms.<sup>6</sup> In this case, the distribution of untransformed iron grades is only slightly negatively skewed and its variogram has a low nugget effect. For this reason, the variograms on the raw and gaussian transformed variables are very similar with the main difference being that the sill of the gaussian transformed variograms is equal to 1.

### Selection of a block size for estimation

Before a search strategy can be optimised, it is standard practice to optimise the parent block size. This would involve a different block size for each dataset. For comparative purposes and to represent

**Table 2 Parameters for the three structure spherical variogram models presented in Fig. 3**

Nugget	1
Range 1, east–west	12
Range 1, north–south	17
Sill 1	17
Range 2, east–west	110
Range 2, north–south	37
Sill 2	26.5



**3 Horizontal directional variograms and their corresponding three structure spherical models. These variograms were generated using all of the blasthole data. D1 is oriented 0° to 090°, D2 0° to 060°, D3 0° to 030°, D4 0° to 000°, D5 0° to 330° and D6 0° to 300°**

the variety of situations often used in estimation, a block model made up of 20 x 20 m blocks is selected. This block model varies from one-quarter the drillhole spacing of the random grid through to the same spacing as the regular grid.

While this example uses small block sizes relative to the random sample grid (common industry practice), this is generally not recommended. Armstrong and Champigny<sup>2</sup> have clearly demonstrated the inherent smoothing caused by kriging into small blocks and warned against using such estimates to calculate recoverable reserves. Demonstrating this over-smoothing is not the intention of this paper, rather the relative performance of various error determination methods for commonly used sample-grid to block-size ratios is investigated.

### Search ellipse optimisation and selection

To implement inverse distance, ordinary kriging and sequential gaussian simulation, the samples relevant to the block being estimated (or the point being simulated) must be determined. Here this is done by estimating via ordinary kriging each 20 x 20 m block with different search ellipse sizes (Table 3) and recording the number of negative kriging weights, the slope of the regression between ‘actual’ and ‘estimated’ grades and the kriging variance.

The above-mentioned statistics are summarised, graphed and the optimal search ellipse is found by determining where increasing the size of the search ellipse does not significantly improve the estimate. More specifically, this is where increasing the size of the search ellipse does not significantly increase the slope of the regression between ‘actual’ and ‘estimated’ grades, decrease the kriging variance and increase the number of negative kriging weights.<sup>14</sup> Fig. 4 represents an example of one such graph for the regular sample grid.

**Table 3 Search ellipse sizes used to optimise the estimates. The E–W and N–S search refers to the maximum distance from the point being estimated. The reference field refers to the data plotted on the X-axis of Fig. 4**

Search reference number	E–W search (m)	N–S search (m)
1	25	12.5
2	25	25
3	50	25
4	50	50
5	75	50
6	75	75
7	100	75
8	100	100
9	150	100
10	150	150
11	200	150
12	200	200
13	250	200
14	250	250
15	300	300

The optimal search ellipse selected for the full data set is 50 x 50 m, for the regular dataset it is 150 x 100 m (east–west and north–south, respectively) and 500 x 300 m (east–west and north–south, respectively) for the random and random stratified data sets.

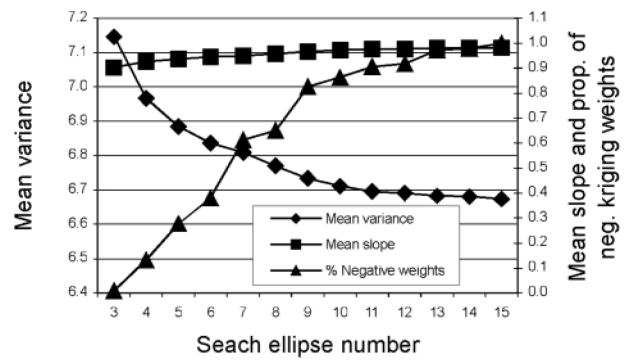
## IMPLEMENTATION AND ANALYSIS OF SIMULATION AND ESTIMATION

### Implementation of the estimation and simulation methodologies

Nearest neighbour, inverse distance squared and ordinary kriging estimations, and sequential gaussian simulations (Table 4) are implemented below.

**Table 4 Comparison of various types of estimates and simulations with the real data. The search reference field refers to the search ellipse documented in Table 5. Nearest neighbour = NN, inverse distance squared = ID2, ordinary kriging = OK, and sequential gaussian simulation = SGS. The mean percentage difference (MPD) is calculated from the estimated or simulated block grade (point simulations averaged into blocks) compared to the real grades on a block by block basis**

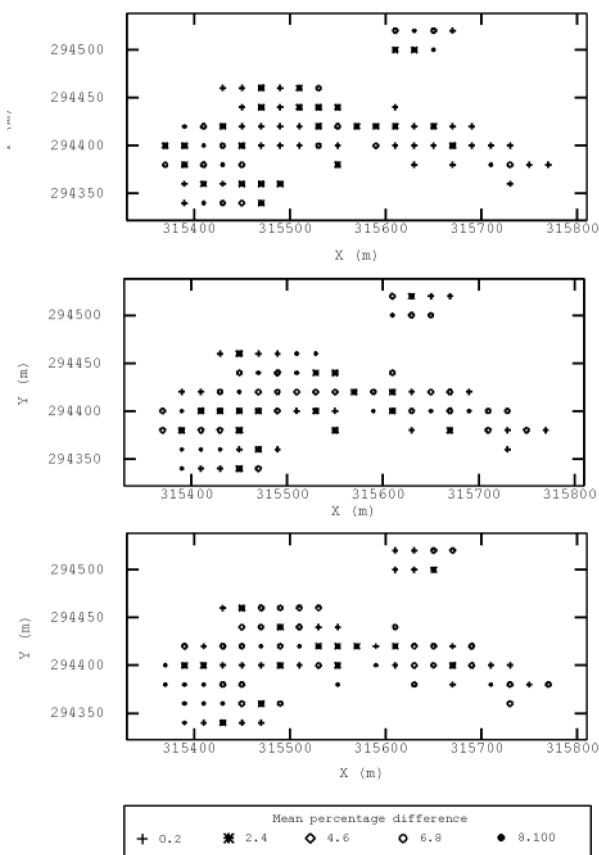
Dataset	Mean % Fe	Sample mean % Fe	MPD	Search reference	Optimal search	Method
All data	58.2	58.4	...	2	Yes	OK
Random	59.6	59.9	5.3	4	Yes	ID2
Random	59.3	59.9	5.1	5	Yes	OK
Random	59.8	59.9	5.4	6	No	ID2
Random	59.9	59.9	5.1	6	No	OK
Random	59.0	59.9	5.7	10	...	NN
Random	59.6	59.9	5.3	2	Yes	SGS
Random stratified	57.4	57.17	4.9	4	Yes	ID2
Random stratified	57.2	57.17	4.7	5	Yes	OK
Random stratified	57.7	57.17	5.5	6	No	ID2
Random stratified	57.9	57.17	4.9	6	No	OK
Random stratified	58.5	57.17	8.2	10	...	NN
Random stratified	57.0	57.17	4.6	5	Yes	SGS
Regular	57.4	57.25	3.5	7	Yes	ID2
Regular	57.4	57.25	3.1	8	Yes	OK
Regular	57.3	57.25	4.5	9	No	ID2
Regular	57.3	57.25	4.3	9	No	OK
Regular	57.5	57.25	7.4	10	...	NN
Regular	57.4	57.25	2.7	8	Yes	SGS



**4 Graph of search ellipse number versus statistics used to optimise the search ellipse size for the regular sample grid. The search ellipse number refers to search ellipse sizes in Table 3 and the search ellipse size increases from left to right. The number of negative kriging weights is obtained by multiplying the proportion by the total number of negative kriging weights (823) for the largest search ellipse**

The ordinary kriging utilises a block representation of 64 discrete points per 20 x 20 m block. The sequential gaussian simulation is based on 50 realisations of points in 1 x 1 m blocks which are re-blocked up to 20 x 20 m blocks.

Octant searching is used for the inverse distance squared interpolation with a minimum of two octants to be filled before a block is estimated and each octant can have a maximum of 8 samples. With the ordinary kriging and sequential gaussian simulation, octant searching is not used as kriging by its nature partially declusters the data.<sup>8</sup>



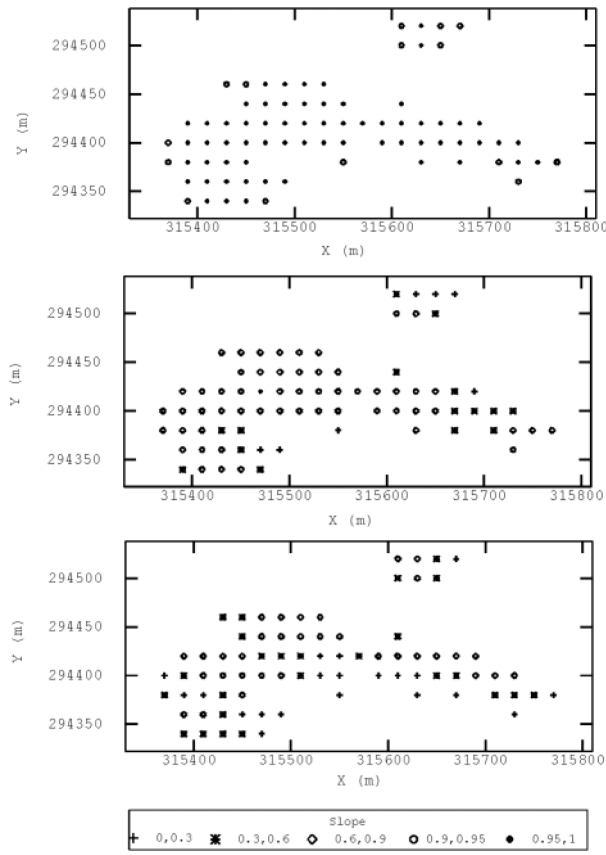
**5 Mean percentage difference of actual percent iron versus the estimated value of blocks estimated via ordinary kriging with an optimal search strategy. The upper plan represents the regular dataset, the middle plan represents the random stratified dataset and the lower plan represents the random dataset**

**Methodology for the comparison between actual and estimated or simulated grades**

Grades for each 20 x 20 m block determined via the ordinary kriging estimate of the full 9 x 15 m (with 1 centre hole) blasthole dataset were assumed to be the true grades. There is a high degree of confidence in this estimate as the slope of the regression between ‘actual’ and ‘estimated’ grades is 99.5 indicating a conditionally unbiased estimate.<sup>12</sup>

**Table 5 Search ellipses used during estimation and simulation. The search reference field refers to the search ellipse documented in Table 4**

Search reference number	E–W search (m)	N–S search (m)	Octant search
1	50	50	Yes
2	50	50	No
3	6	6	Yes
4	500	300	Yes
5	500	300	No
6	50	50	Yes
7	150	100	Yes
8	150	100	No
9	20	20	Yes
10	1000	1000	No



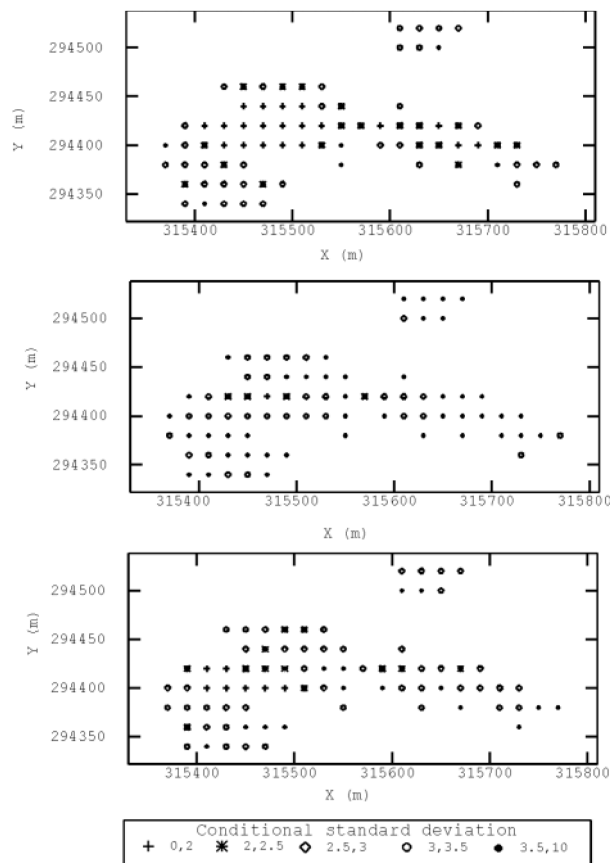
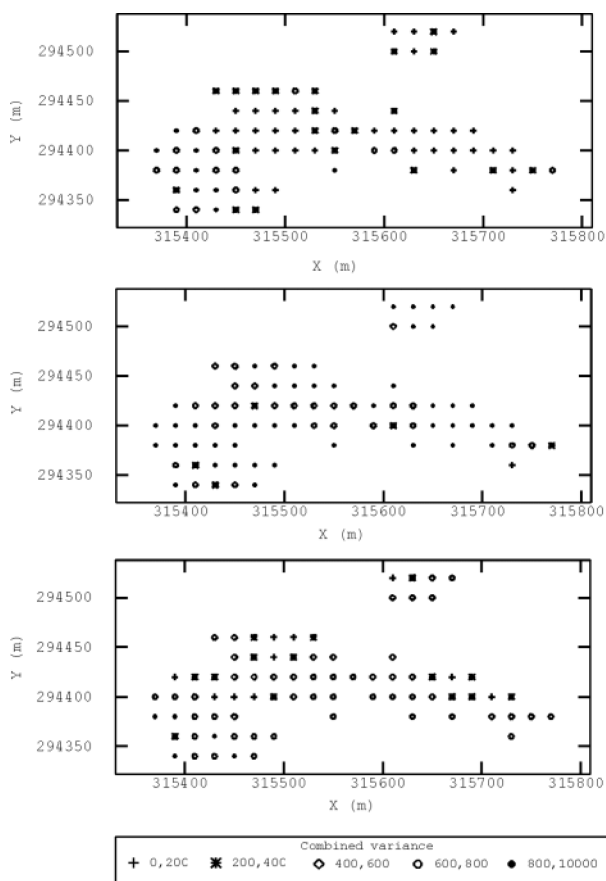
**6 Slope of the regression between ‘actual’ and ‘estimated’ grades of blocks estimated via ordinary kriging with an optimal search strategy. The upper plan represents the regular dataset, the middle plan represents the random stratified dataset and the lower plan represents the random dataset**

The mean grade of the actual estimate is compared against estimates or simulations based on the data subsets. Here, the mean grade of the sample data must be kept in mind, as this will limit the ability of the various techniques to determine the actual mean grade.

The actual block grades are compared against the grades obtained via the various data subsets and estimation or simulation methodologies (Table 4). This comparison is done via the mean percentage difference (actual versus the estimate or the actual versus the average of multiple simulations) of all the 20 x 20 m blocks. This is not a comparison of the global mean but of the average of block-by-block comparisons. In this way, the conditional bias of the estimates or simulations are measured, with a low mean percentage difference indicating less conditional bias.

**Discussion of the results**

Nearest neighbour estimation consistently provides the highest mean percentage difference of the actual percent iron versus the estimated value (Table 4); however, the mean grade of the nearest neighbour estimates is relatively close to the actual grade. This indicates that, while the block-by-block estimates are conditionally biased, the nearest neighbour estimation effectively declusters the data providing an acceptable global estimate of the mean.



**7 Combined variance for blocks estimated via ordinary kriging with an optimal search strategy. The upper plan represents the regular dataset, the middle plan represents the random stratified dataset and the lower plan represents the random dataset**

**8 Conditional standard deviation of 50 realisations produced via sequential gaussian simulation. The upper plan represents the regular dataset, the middle plan represents the random stratified dataset and the lower plan represents the random dataset**

The nearest neighbour technique is useful for declustering data and if a small block size is used it will produce comparable results to a polygonal declustering.

As might be expected, the best performing linear-estimate is ordinary kriging with an optimal search strategy. The use of a non-optimal search strategy in ordinary kriging downgrades the quality (mean percentage difference and global mean) of the estimates significantly. The inverse distance interpolation with a non-optimal search strategy performs poorly both in terms of mean percentage difference (actual percent iron versus the estimated value) and the global mean grade. The above-mentioned results show that an optimal search strategy is critical for good interpolation and that the benefits of ordinary kriging over inverse distance can be negated by a poor search strategy.

It is a common misconception that the average of many simulations will provide the same results as ordinary kriging. As indicated by Guibal<sup>6</sup> and Dimitrakopoulos,<sup>4</sup> the ordinary kriging estimate and average of many simulations will not necessarily be identical. In this case study, the global means from sequential gaussian simulation are similar but different from ordinary kriging. As suggested by Guibal.<sup>6</sup> In this case, the difference is probably due to the fact that simulation works with a strong stationarity hypothesis;

therefore, the mean grade of the samples will be very similar to the mean grade of the multiple simulations.

The mean percentage difference (actual percent iron versus the average of multiple simulations) is significantly lower than the other estimates for the regular dataset and slightly lower for the random stratified dataset. This is probably because the simulation does not over-smooth the 20 x 20 m block grades. For the random dataset, the sequential gaussian simulation does not perform better than the other methods. This is because this dataset has the least number of samples and thus the gaussian transform is poorly defined. If a larger random dataset was used, it would be expected that the sequential gaussian simulation would out-perform other methods in terms of mean percentage difference (actual percent iron versus the average of multiple simulations).

One common approach to classifying resources is based on using multiple search sizes during interpolation. Blocks not filled by the smallest search ellipse are re-estimated with a larger search ellipse; finally, those blocks not filled by the first two ellipses are estimated with a still bigger search ellipse. The resource is then classified according to the pass number as inferred, indicated or measured.<sup>9</sup> One problem with this approach is that it is often applied without selecting an optimal search for the first pass. This results in sub-optimal interpolation.

## BLOCK GRADE ERROR ESTIMATION

### A spatial comparison of actual error to error obtained from estimation or simulation

Fig. 5 represents plans of the mean percentage difference of the actual versus estimated iron grades. This can be compared with the error estimated by the slope of the regression between ‘actual’ and ‘estimated’ grades (Fig. 6) the combined variance (Fig. 7) and the conditional standard deviation of 50 simulations (Fig. 8).

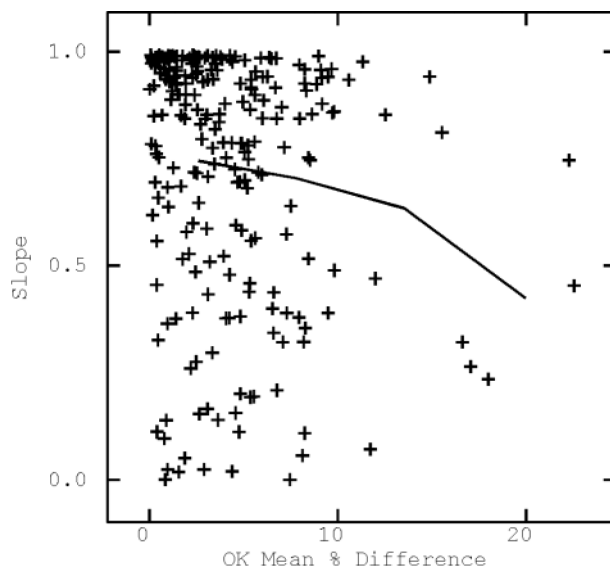
The estimated slope of the regression between ‘actual’ and ‘estimated’ grades (Fig. 6) will produce comparable spatial results to other error estimators such as kriging variance and kriging efficiency, which take into account the spatial relationship of the samples relative to the block being estimated. As could be expected, for the regular spaced dataset, the slope of the regression between ‘actual’ and ‘estimated’ grades indicates highest error around the edges of the domain, which intuitively is reasonable.

The combined variance (Fig. 7) and the conditional standard deviation include grade information as well as spatial information in estimating or simulating uncertainty. Because of this characteristic, the spatial distribution of errors based on these methodologies is different to spatially based error estimates such as the kriging variance.

As can be seen by Figs. 5–8, there appears to be little or no spatial relationship between the errors obtained from estimation or simulation and the actual errors. This is partially because the kriging variance and the conditional standard deviation represent the distribution of errors for a block and statistically the observed single error is simply one possible realisation from this distribution.

### A statistical comparison of actual error to error obtained from estimation or simulation

Because a clear relationship between errors obtained from estimation or simulation and actual errors is difficult to visualise, another way must be chosen to evaluate the various error determination methodologies. As presented in Fig. 9, we have chosen to plot scatter-plots of mean percentage difference (actual percent iron versus the estimated value or the actual versus the average of multiple simulations) versus the error estimate



**9 Slope of the regression between ‘actual’ and ‘estimated’ grades versus mean percentage difference (actual percent iron versus the estimated value). The dark line is a conditional expectation curve of the data plotted. The conditional expectation curve is obtained by partitioning the values of one scatterplot axis into regular sized bins. For each of these bins the other scatterplot variable is averaged and thus the best-fit line obtained**

or the conditional standard deviation. These plots are not all presented below, but they are summarised in Table 6 via correlation coefficients. One additional benefit of these scatter-plots is that they are a calibration of the error determined from estimation or simulation with the actual error.

Of the error estimates possible for inverse distance interpolation, the number of samples provides the highest correlation with mean percentage difference (actual percent iron versus the estimated value). In this situation, the number of samples within the optimised search gives an indication of the spatial distribution of the samples through the use of octant searching. Without an optimal search ellipse or octant

**Table 6 Correlation coefficients of various error determination methodologies versus the mean percentage difference (actual percent iron versus the estimated value or actual versus the average of multiple simulations). The ordinary kriging, simulation and inverse distance weighting all utilise optimal search ellipse sizes**

Error estimate	OK	SGS	ID2
Weighted actual distance	0.1823	...	0.1113
Weighted transformed distance	0.0951	...	-0.0421
Weighted average variogram	0.2186	...	...
Slope	-0.1701	...	...
Combined variance	0.2025	...	...
Transformed distance to closest sample	0.0739	...	0.1126
Kriging efficiency	-0.2222	...	...
Non-transformed distance to closest sample	0.1157	...	0.1298
Kriging variance	0.2222	...	...
Number of samples	...	...	-0.2527
Conditional standard deviation	...	0.20	...



searching this method would not perform as well. For regular spaced sample grids, the distance to the nearest sample (drillhole spacing) would produce similar results to the number of samples.

For ordinary kriging estimates, the kriging variance, kriging efficiency and the slope of the regression between 'actual' and 'estimated' grades all perform comparatively well and these are the most commonly accepted measures of error used in ordinary kriging.<sup>12</sup> The conditional standard deviation from sequential gaussian simulation is similar (correlation with the actual error) to the kriging variance. The weighted average variogram also performs well, but is less commonly used for error estimation than kriging variance or simulation.

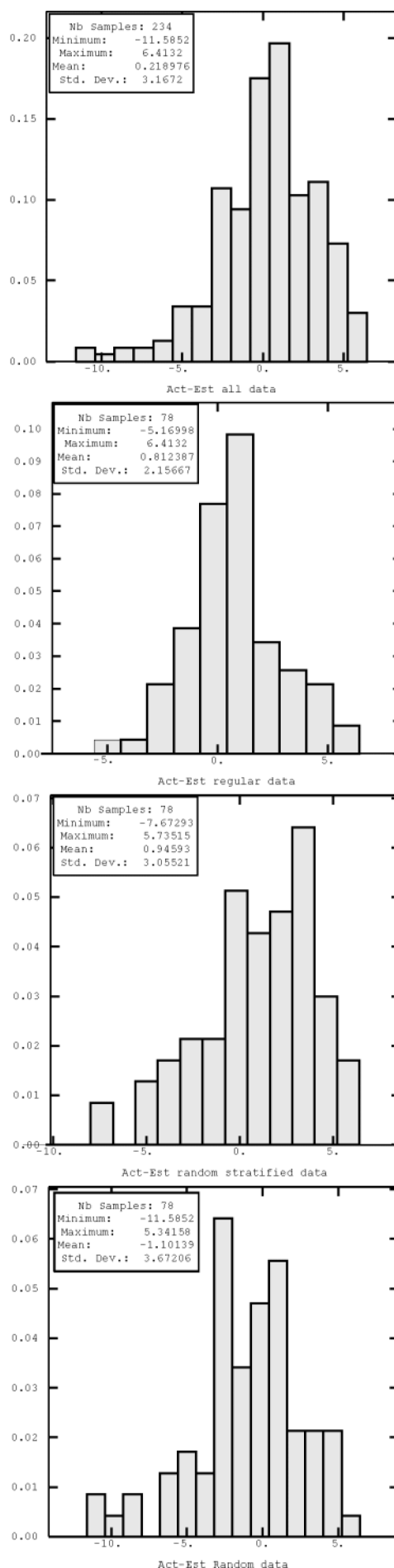
The combined variance has performed well and may out-perform the other error estimation methods in highly skewed distributions where the domains are not completely stationary. This is because the method takes into account the spatial as well as grade information. However, in areas of poor stationarity, perhaps a non-linear interpolation would be more appropriate than ordinary kriging.<sup>17</sup>

## ASSUMPTIONS ON THE DISTRIBUTION OF ERRORS

One of the benefits of conditional simulation is that a full distribution of possible grades or possible errors can be generated for each block being simulated. With kriging variance, we have the variance of the distribution of errors but we do not know the shape of the error distribution. Thus, in order to classify blocks according to confidence limits,<sup>13</sup> assumptions must be made about the shape of the distribution of errors. Typically, the chosen error distribution is gaussian; however, the assumption of a gaussian distribution will not fit perfectly with iron grades, as the maximum possible iron grade is 70% and the distribution is negatively skewed.

To understand better the shape of the distribution of errors (for the ordinary kriging estimate), we have subtracted the actual percent iron from the ordinary kriging (optimal search) estimated iron and plotted histograms of this data for the three data subsets (Fig. 10). Rather than accepting a gaussian distribution of errors, we can assume that the shape of these histograms is representative of individual block error distributions. For each ordinary kriging block estimate, we have a kriging variance and a mean error of zero. With the above assumption of the skewness of the distribution, we have fully described the distribution of errors for each block. It should be kept in mind that, because the

**10 Histograms of the actual percent iron grades minus the ordinary kriged block estimates. The upper histogram represents the combined regular, random stratified and random datasets, the upper-mid histogram represents the regular dataset, the lower-mid histogram represents the random-stratified dataset and the lower histogram represents random dataset**



mean grades of the data subsets are different to the actual data, this could bias the results. In this case, the conclusions are considered representative due to the nature of the mineralisation (*i.e.* negatively skewed with a maximum iron grade of 70%).

The following example of a hypothetical kriged block estimate of 59% Fe and a kriging variance of 10 illustrates how we can use the above-mentioned information. If we assume that the distribution of errors for this hypothetical block is gaussian, we would have a mean error (actual–estimate) of  $0.0 \pm 6\%$  Fe at 95% confidence; however, the error assuming a slightly negatively skewed error distribution would be  $0.0 \pm 5\text{--}8\%$  Fe at 95% confidence.

## LIMITATIONS AND NEXT STEPS

### Definition of grade boundaries

The error estimation and simulation methodologies used above can only partially account for the error in the definition of the grade boundary. In this study, the grade boundary was the same for all datasets; however, as described by Stegman,<sup>16</sup> the error in the definition of the grade boundary will often be greater than the error in the estimation of grades. Grade boundary error can be determined in various ways such as, indicators, simulations, removing data<sup>7</sup> and simple mathematical formulas.<sup>3</sup>

### Data selection

Although the use of the two-dimensional dataset should not significantly affect the comparison of techniques presented in this paper, estimated and simulated block grades would be less accurate than if a full three-dimensional data set had been used.

In using blasthole data without modification, we assume that the difference in nugget and the sample support between blastholes and drillholes is not great. In addition, there is assumed to be no bias in either drillhole or blasthole data.

Only iron was used in this study; however, in general, several of the major contaminants such as aluminium, silica and phosphorus would need to be studied before making conclusions about resource classification. Typically, the most variable and risky element would be the basis for the resource classification.

The three datasets contain different numbers of samples and different mean grades. The grids were selected to be comparable to actual examples on site. In these examples, the mean grade of the samples are quite different from the actual grades. It could be argued that for a more valid comparison between methods that each dataset should have had a similar number of samples with similar mean grades. This would minimise the potential for results to be biased by using datasets with different mean grades.

Another approach towards better understanding the limits of the data selected would be to re-select (several times) the three sample grids with the same

number of samples and from the same parent dataset. It may be found that this approach gives a better estimate of uncertainty than what has been presented in this paper.

### Variography

One variogram based on the full dataset was used for all data subsets. This could be argued as being overly favourable for the ordinary kriging estimate; however, in a typical mining situation (where drillhole spacing is significantly wider than the blasthole data) due to the presence of blasthole data, the variogram is generally well known. Uncertainty in the variogram definition could be investigated by repeating the above study with variograms representing maximal and minimal plausible continuity.

### Resource classification

Authors have used various techniques to convert simulations or estimated error into resource classifications. For example, Krige<sup>12</sup> proposed that a block kriging efficiency less than 0.3 is inferred, 0.3–0.5 is indicated and above 0.5 is measured. Mwasinga<sup>13</sup> provided more examples of how the various error estimation methodologies can be used to classify individual blocks.

While classifying individual blocks is a necessary step, these classifications are not the final step. If individual blocks are classified, unrealistic classifications such as bulls-eyes around data can result. The individual blocks must be grouped into zones of similar confidence. This can be done visually with wire-framing or mathematically via erosion and dilation. Once blocks are grouped, the error of realistic production tonnages (*e.g.* 1 year's production) can be estimated or obtained from the analysis of multiple simulations. To estimate the error of combined blocks, the two-dimensional estimation technique of Journel and Huijbregts<sup>10</sup> can be used. This technique takes into account error in grade estimation, grade boundary location, tonnage and specific gravity. Ideally, production data would also be available for calibration. Initially, this work can be time consuming, as it requires several iterations to determine the appropriate individual block classifications.

## CONCLUSIONS

The global mean iron grade of averaged multiple simulations and all estimation methods was similar. With individual blocks the average of multiple simulations generally reproduced most closely the actual grades and of the linear estimators ordinary kriging outperformed inverse distance and nearest-neighbour estimations.

Unless ordinary kriging uses an optimal search routine, the results will be little or no better than a well-implemented inverse-distance weighting estimate. Thus, resource classification based on different blocks being estimated by different sized search ellipses should only be used with an optimal search strategy.

Of the error estimation methodologies for inverse-distance squared interpolation, the number of samples

used in octant searching produced the most accurate estimates of errors. However, this technique is highly dependent on an optimal search strategy. Of the error estimation techniques used in kriging, kriging variance, kriging efficiency and the slope of the regression between 'actual' and 'estimated' grades generally out-performed other techniques. In domains with poor stationarity, the combined variance may out-perform other ordinary kriging-based error estimates that only take into account the spatial location of samples. The conditional standard deviation from sequential gaussian simulation produced comparable results to the kriging variance.

The small number of samples used limits all of the above-mentioned grade estimation techniques and the sequential gaussian simulation. This is because if the input data are not representative, no estimation or simulation technique will compensate for this. However, in this case study, higher and lower grades than the input data were permitted in the back transformation from gaussian values. This resulted in the simulation containing some grades higher and lower than the sample data. Despite this positive characteristic of simulation, the random and random-stratified datasets used were too small to implement simulation properly. This is because the assumption of stationarity is even stronger in simulation than for ordinary kriging. Also, a meaningful histogram (to gaussian transform grades) could not be obtained from 10–20 samples.

The benefit of better understanding the shape of the distribution of errors for kriging estimates was demonstrated and the dangers of assuming a gaussian distribution of errors emphasised. Finally, the error determined for individual blocks needs to be classified and combined into groups of blocks that form packages of meaningful size to the mining operation. Ultimately, it is these groups of blocks, and not individual blocks, that are classified according to the JORC<sup>9</sup> criteria.

This study demonstrates the performance of sequential gaussian simulation and various grade and error estimation methodologies in the study area. As a result of these findings, the competent person can determine better which of these methods is appropriate for his or her purpose.

## ACKNOWLEDGEMENTS

The permission of BHP Billiton to publish this paper is greatly appreciated, as is the technical support of D. Guibal, G. Yeates, J. Macdonald and M. Kneeshaw are thanked for their review and constructive criticism of this document.

This paper was originally presented at the Australasian Institute of Mining and Metallurgy (AusIMM) and CSIRO conference *Iron Ore 2002* held at Perth, Western Australia, on 9–11 September 2002, the proceedings of which have been published as a CD-ROM (ISBN 1-875776-94-X, *Miner. Abstracts* 03M/0093).

## REFERENCES

1. A. ARIK: 'Uncertainty, confidence intervals and resource categorization: a combined variance approach', Proc. ISGSM, Perth, Australia, 1999.
2. M. ARMSTRONG and N. CHAMPIGNY: 'A study on kriging small blocks', *Can. Min. Metall. Bull.*, 1989, **82**, 128–133.
3. M. DAVID: 'Developments in geostatistics 2, Geostatistical ore reserve estimation', Amsterdam, Elsevier, 1977, 1–364.
4. R. DIMITRAKOPOULOS: Personal communication, April 2002.
5. D. GUIBAL: 'Variography, a tool for resource geologist', (ed. A. C. Edwards), Mineral Resource and Ore Reserve Estimation – The AusIMM Guide to Good Practice, Melbourne, AusIMM, 2001, 85–90.
6. D. GUIBAL: Personal communication, May 2002.
7. M. HUMPHREYS: 'A case study testing estimation sensitivity to data in an Australian gold deposit', (eds. W. J. Kleingeld, D. G. Krige), Geostats 2000, Vol 2, Cape Town, Geostatistical Association of South Africa, 2000, 724–731.
8. E. H. ISAACS and R. M. SRIVASTAVA: 'Applied geostatistics', Oxford, Oxford University Press, 1989, 1–561.
9. JORC: 'Australasian code for reporting of mineral resources and ore reserves (the JORC code)', The Joint Ore Reserves Committee of the Australasian Institute of Mining and Metallurgy, Australian Institute of Geoscientists and Minerals Council of Australia, Melbourne, AusIMM, 1999, 1–17.
10. A. G. JOURNEL and C. H. J. HUIJBREGTS: 'Mining geostatistics', New York, Academic Press, 1978, 1–600.
11. M. KNEESHAW: 'Guide to the geology of the Hamersley and North East Pilbara Iron Ore Provinces', BHP Billiton, unpublished report, 2000.
12. D. G. KRIGE: 'A practical analysis of the effects of spatial structure and of data available and accessed on the conditional biases in ordinary kriging', (eds. E. Y. Baafi, N. A. Schofield), Geostatistics Wollongong 1996, Amsterdam, Kluwer, 1996, 719–810.
13. P. MWASINGA: 'Approaching resource classification: general practices and the integration of geostatistics', (eds. Xie, Wang, Jiang), Computer applications in the minerals industries, New York, Lisse, 2001, 97–104.
14. J. RIVOIRARD: 'Two key parameters when choosing the kriging neighbourhood', *Math. Geol.*, 1987, **8**, 851–856.
15. D. V. SNOWDEN: 'Practical interpretation of mineral resource and ore reserve classification guidelines', (ed. A. C. Edwards), Mineral resource and ore reserve estimation – the AusIMM guide to good practice, Melbourne, AusIMM, 2001, 643–652.
16. C. L. STEGMAN: 'How domain envelopes impact on the resource case studies from the Cobar Gold Field, NSW, Australia', (ed. A. C. Edwards), Mineral resource and ore reserve estimation – the AusIMM guide to good practice, Melbourne, AusIMM, 2001, 221–236.
17. J. VANN and D. GUIBAL: 'Beyond ordinary kriging – an overview of non-linear estimation', (ed. A. C. Edwards), Mineral resource and ore reserve estimation – the AusIMM guide to good practice, Melbourne, AusIMM, 2001, 249–256.

## Author

**Chris De-Vitry** developed a love for geology very early in life, as his father was a prospector and small-scale miner. However, after 12 months underground at the business end of a shovel, he was convinced study would be a good option. In 1992, he completed a BSc in Geology at the Australian

National University and was subsequently employed by WMC Resources as a junior geologist at the Redeemer underground gold mine and the Cox open pit near Leinster, Western Australia. In 1994, he returned to study and completed an Honours in Geology at the University of Western Australia, and in 1995 returned to WMC Resources as underground mine geologist at the Rocky's Reward underground nickel mine near Leinster. During this time, he completed a part-time MSc in Ore Deposit Geology and Evaluation at the University of Western Australia. From

1997 to 2000, he worked for WMC Resources as a resource geologist in Melbourne, Canada, Cuba and Perth; but, after several major projects closed, was transferred to the Three Springs open pit Talc Mine which was subsequently sold. During the sale process, he accepted a position as a resource geologist at BHP Billiton's iron ore operations at Newman where he has been for the last 18 months. He has been promoted to senior resource geologist and will soon be moving to MPI Mines, Stawell Gold Mine, P.O. Box 265 Stawell, 3380, Victoria, Australia.